PCCP

PAPER

View Article Online
View Journal | View Issue

Cite this: *Phys. Chem. Chem. Phys.*, 2020, **22**, 13698

Trends in stabilisation of Criegee intermediates from alkene ozonolysis†

Mike J. Newland, *[a] Beth S. Nelson, [a] Amalia Muñoz, [b] Milagros Ródenas, [b] Teresa Vera, [b] Joan Tárrega [b] and Andrew R. Rickard [ac]

Criegee Intermediates (CI), formed in the ozonolysis of alkenes, play a central role in tropospheric chemistry as an important source of radicals, with stabilised CI (SCI) able to participate in bimolecular reactions, affecting climate through the formation of inorganic and organic aerosol. However, total SCI yields have only been determined for a few alkene systems, while speciated SCI yields from asymmetrical alkenes are almost entirely unknown. Here we report for the first time a systematic experimental exploration of the stabilisation of CH_2OO and $(CH_3)_2COO$ CI, formed from ten alkene–ozone systems with a range of different sizes and structures, under atmospherically relevant conditions in the EUPHORE chamber. Experiments in the presence of excess SO_2 (an SCI scavenger) determined total SCI yields from each alkene–ozone system. Comparison of primary carbonyl yields in the presence/absence of SO_2 determined the stabilisation fraction of a given CI. The results show that the stabilisation of a given CI increases as the size of the carbonyl co-product increases. This is interpreted in terms of the nascent population of CI formed following decomposition of the primary ozonide (POZ) having a lower mean energy distribution when formed with a larger carbonyl co-product, as more of the energy from the POZ is taken by the carbonyl. These findings have significant implications for atmospheric modelling of alkene ozonolysis. Higher stabilisation of small CI formed from large alkenes is expected to lead to lower radical yields from CI decomposition, and higher SCI concentrations, increasing the importance of SCI bimolecular reactions.

Received 17th February 2020,
Accepted 4th June 2020

DOI: 10.1039/d0cp00897d

rsc.li/pccp

Introduction

The formation of Criegee intermediates (CI) from gas phase alkene ozonolysis has received attention over the past five decades owing to their role as important non-photolytic sources of radicals (OH, HO_2 and RO_2) to the troposphere.[1–5] More recently, the potential importance of bimolecular reactions of stabilised CI (SCI) has been the subject of much research (see Vereecken *et al.*[6] and references within). These reactions contribute significantly to the sulfuric acid budget in certain environments through oxidation of SO_2,[7] and the acidity of the atmosphere through removal of organic and inorganic acids.[8] Bimolecular reactions of SCI have also been implicated in the formation of aerosol from monoterpene ozonolysis[9] through dimerization,[10,11] oligomerization[12] and reaction with peroxy radicals,[13] contributing to new particle formation[14] and so directly affecting cloud condensation nuclei,[15,16] rainfall, and climate.

The Criegee ozonolysis reaction mechanism[17] proceeds *via* concerted cycloaddition of the ozone molecule across the C=C double bond to form a chemically activated primary ozonide (POZ), followed by cleavage of the C–C bond and one of the O–O bonds forming a carbonyl molecule and a carbonyl oxide, or 'Criegee intermediate',[18] see Scheme 1. A population of ozonolysis derived CIs in the gas-phase is formed with a broad internal energy distribution.[19] A fraction of CI may be formed 'cold' (although this is not the case for all alkenes[20,21]), that is, without enough internal energy to undergo prompt decomposition, these are termed stabilised Criegee intermediates (SCI). The remainder are formed chemically activated (CI*). These CI* tend to undergo prompt decomposition on a timescale of nanoseconds.[22] However, they can also be collisionally deactivated to add to the SCI population. The distinction between these two routes to SCI formation has been demonstrated in laboratory experiments performed as a function of pressure.[20,21,23–25] The fraction of each type of CI that is formed will depend on the initial energy distribution of the CI population.[24]

Unimolecular decomposition of CI yields a range of radical products, with decomposition of *syn*-CI (*i.e.* CI with an alkyl

[a] *Wolfson Atmospheric Chemistry Laboratories, Department of Chemistry, University of York, UK. E-mail: mike.newland@gmail.com*
[b] *Fundación CEAM, EUPHORE Laboratories, Avda Charles R. Darwin 14. Parque Tecnológico, Valencia, Spain*
[c] *National Centre for Atmospheric Science, Wolfson Atmospheric Chemistry Laboratories, University of York, UK*

† Electronic supplementary information (ESI) available. See DOI: 10.1039/d0cp00897d

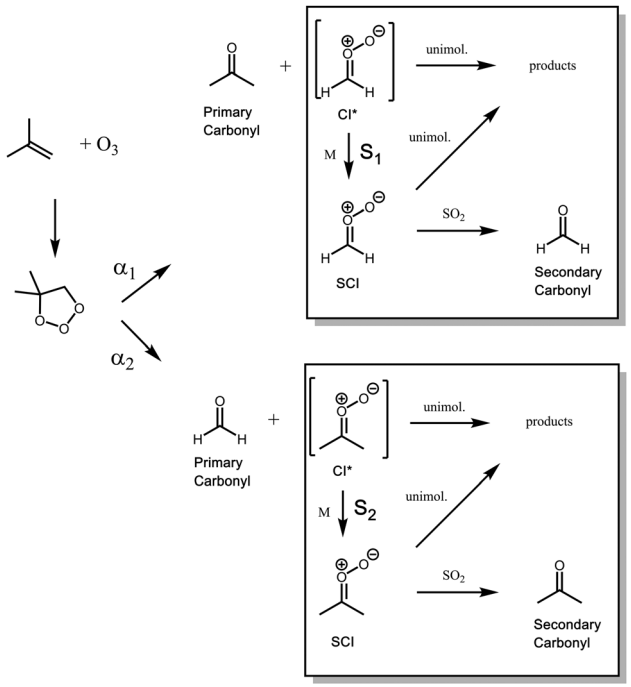

Scheme 1 Simplified mechanism for the production of CI and primary and secondary carbonyl products in the ozonolysis of 2-methyl propene.

group on the same side of the terminal O atom of the carbonyl oxide moiety), *via* a vinyl hydroperoxide, producing OH with (near) unit yield. SCI can have sufficiently long lifetimes to undergo bimolecular reactions with H_2O, RCOOH, and SO_2, amongst other species, in the atmosphere. Hence the relative yields of CI/SCI from a particular alkene–ozone system determine the effect of that system on atmospheric composition.

Inclusion of alkene ozonolysis chemistry in regional and global chemical transport models is essential to correctly estimate radical concentrations, and the product distribution from the removal of alkenes by reaction with ozone. However, such mechanisms must firstly parameterize SCI yields for a structurally diverse range of alkenes for which no measurements exist, lumping together SCI of different structures and hence reactivities, and secondly lumping together stabilisation of different SCI. This leads to large uncertainties on the SCI yields and hence on the effect of alkene–ozone reactions on atmospheric composition.

Many laboratory studies probing the chemistry of SCI have utilised the facile photolysis of alkyl iodides to yield SCI in the presence of oxygen.[26] This has proved an invaluable resource for the study of SCI chemistry. However, alkene ozonolysis is expected to be the dominant source of CI to the atmosphere, and certain atmospherically relevant questions, such as the fractional CI and SCI yields from alkene ozonolysis, can only be answered by probing the alkene–ozone system.

Total SCI yields have previously been measured from a number of atmospherically relevant alkene–ozone systems including short chain alkenes,[27–31] isoprene,[32–34] and monoterpenes.[7,32] These yields are generally measured indirectly, either by the removal of an SCI scavenger (*e.g.* SO_2) or formation of a product from an SCI scavenging reaction (*e.g.* production of H_2SO_4, *via* the SO_2 + SCI reaction). However, very little experimental information exists on the relative amounts of different SCI formed in non-symmetrical systems. For non-symmetrical, non-cyclic, alkenes, a pair of CI and carbonyl co-products are formed (Scheme 1). The yield of each SCI depends on: (i) the yield of each CI – determined by the fragmentation of the POZ (α); (ii) the fraction of each CI that is stabilised (S). The stabilisation of a given CI produced from different alkene–ozone systems might be expected to differ. For example, while the fraction of CH_2OO stabilised in ethene ozonolysis has been determined to be 0.35–0.54 based on a wide range of experimental studies, the chamber studies of Nguyen *et al.*[34] suggest that the majority of CH_2OO formed in isoprene ozonolysis is stabilised.

Here, we present results of a series of alkene ozonolysis experiments carried out at the European PhotoReactor facility (EUPHORE), Valencia, Spain, in which yields of chemically activated and stabilised CH_2OO and $(CH_3)_2COO$ are determined, for the first time, for a systematic range of alkene–ozone systems under atmospherically relevant conditions. An empirical structure–activity relationship for the stabilisation of these types of Criegee intermediates, based on the size of the carbonyl co-product formed in the decomposition of the primary ozonide is also presented, with the atmospheric implications of the results discussed.

Experimental

EUPHORE

EUPHORE is a 200 m^3 simulation chamber used for studying reaction mechanisms under atmospheric boundary layer conditions. The chamber is fitted with large horizontal and vertical fans to ensure rapid mixing (three minutes). Further details of the chamber setup and instrumentation are available elsewhere.[35–37] Experiments comprised time-resolved measurement of the formation of carbonyl products and the loss of alkene and ozone (and in some experiments SO_2). SO_2 and O_3 abundance were measured using conventional fluorescence and UV absorption monitors, respectively; alkene and oxygenated volatile organic compound abundance was determined *via* FTIR spectroscopy and PTR-MS. The precision of the SO_2 and O_3 monitors were 0.25 and 0.47 ppbv respectively (evaluated as 2 standard deviations of the measured value prior to SO_2 or O_3 addition). Experiments were performed in the dark (*i.e.*, with the chamber housing closed; $j(NO_2) \leq 10^{-6}$ s^{-1}), at atmospheric pressure (*ca.* 1000 mbar) and temperatures between 297 and 305 K, on timescales of *ca.* 30–90 minutes. Chamber dilution was monitored *via* the first order decay of an aliquot of SF_6, added prior to each experiment. Cyclohexane (*ca.* 75 ppmv) was added at the beginning of each experiment to act as an OH scavenger, such that SO_2 reaction with OH was calculated to be $\leq$1% of the total chemical SO_2 removal in all experiments.

Experimental approach

Experimental procedure comprised addition of SF_6 and cyclohexane, followed by O_3 (*ca.* 1000 ppbv for the experiments with

alkenes producing CH_2OO, which generally have reaction rates with ozone $\sim 1 \times 10^{-17}$ cm^3 s^{-1}; and *ca.* 500 ppbv for the experiments with alkenes producing $(CH_3)_2COO$, which generally have reaction rates with ozone $\sim 1 \times 10^{-16}$ cm^3 s^{-1}) and SO_2 if used (*ca.* 2000 ppbv). A gap of five minutes was left prior to addition of the alkene, to allow complete mixing. The reaction was then initiated by addition of the alkene (*ca.* 800 ppbv for the systems producing CH_2OO, and 400 ppbv for those producing $(CH_3)_2COO$). The chamber was monitored for 30–90 minutes subsequent to the addition of the alkene depending on the rate of reaction with ozone, the rate of alkene/ozone consumption being dependent on k(alkene + ozone). Roughly 50% of the CH_2OO producing alkenes were consumed after 60 minutes, while 90% of the faster reacting alkenes were consumed within roughly 25 minutes. The experiments were performed under dry conditions (RH < 1%). A full experiment list is given in Table S1 (ESI†).

Results and discussion

Total SCI yields

Alkene ozonolysis experiments were performed in the presence of *ca.* 2000 ppbv SO_2, such that the overwhelming majority (≥94%) of the SCI was scavenged and converted to a carbonyl. The total SCI yield, ϕ, was calculated by regressing the loss of ozone (dO_3) against the loss of SO_2 (dSO_2) (eqn (E1)), both corrected for chamber dilution. In reality the experimentally determined value of ϕ is a minimum value, ϕ_{min} since other loss channels for the SCI (*e.g.* decomposition) may still be having a small but non-negligible effect (Newland *et al.* (2015a)), accounted for in eqn (E1) by f.

$$\frac{dSO_2}{dO_3} = \phi_{SCI\text{-}tot} \cdot f = \phi_{SCI\text{-}min} \quad (E1)$$

In addition to the presence of SO_2 as a potential SCI reaction partner in the chamber, there is also H_2O (<1% RH), HCOOH (of the order of 10 ppbv produced in the ozonolysis reaction), and carbonyls on the order of a few hundred ppbv. For stabilised CH_2OO, decomposition is slow (0.1 s^{-1}, IUPAC) and the only other potentially significant loss process under the experimental conditions employed was bimolecular reaction with water vapour or HCOOH. Based on the IUPAC[38] recommended rate constants, 2000 ppbv of SO_2 is estimated to scavenge >98% of CH_2OO at RH = 1% and [HCOOH] = 10 ppbv (typical mixing ratio present in the chamber for the experimental conditions). For $(CH_3)_2COO$ the only other important loss process under the experimental conditions employed was unimolecular decomposition. 2000 ppbv of SO_2 is estimated to scavenge 94% of $(CH_3)_2COO$ at 303 K based on the IUPAC (IUPAC) recommended rates of $k((CH_3)_2COO + SO_2) = 4.2 \times 10^{-13} \exp^{(1761/T)}$ cm^3 s^{-1} and $k_{uni}((CH_3)_2COO) = 1.0 \times 10^7 \exp^{(-3020/T)}$ s^{-1}. A range of other *syn*- and *anti*-CI will be formed as co-products for many of the alkenes studied here. Using *syn* and *anti*-CH_3CHOO as surrogates, under the experimental conditions employed here, 88% of *syn*-CI will be scavenged by 2000 ppbv SO_2, and 97% of *anti*-CI will be scavenged. Elsamra *et al.*[39] determined $k(CH_2OO + acetone) = 3.0\ (\pm 1.0) \times 10^{-13}$ cm^3 s^{-1} and $k(CH_2OO + acetaldehyde) = 1.2\ (\pm 0.3) \times 10^{-12}$ cm^3 s^{-1}, at 298 K. Products of the reaction are believed to be the carbonyl + acid (*e.g.* $CH_2OO + CH_3CHO \rightarrow CH_3COOH + HCHO$ or $HCOOH + CH_3CHO$), formed *via* decomposition of a secondary ozonide.[40] At 200 ppbv of the carbonyl, this would lead to a sink for CH_2OO of the order of 1–10 s^{-1}, <1% in SO_2 scavenger experiments. Other potential SCI sinks, such as self-reaction are negligible under our experimental setup.

Total SCI yields were calculated for ten alkene–ozone systems in this work (C_2–C_{10}). Fig. 1 shows an example plot of ΔSO_2 *vs.* ΔO_3 for an ozonolysis experiment with 2,4-dimethyl-pent-2-ene. Uncertainties are $\pm 2\sigma$ and represent the combined systematic (estimated measurement uncertainty) and precision components. Fig. S1 (ESI†) shows total SCI plots for each of the ten alkenes studied. Table 1 gives the total SCI yields corrected for additional SCI losses, *i.e.* f, (see Tables S2 and S3, ESI† this correction generally increased the yields by ~5%) calculated for each alkene, and values previously reported in the literature where available.

For alkenes for which total SCI yields have been measured previously, there is good agreement between the values measured here and those reported in the literature. The ethene–ozone system is the most studied, with reported SCI yields ranging from 0.35–0.54, from a range of different techniques – see Newland *et al.*;[31] Alam *et al.*[36] for further references. The value of 0.43 (±0.02) derived here lies towards the lower end of this range. For propene only two values exist in the literature. The value of 0.28 (±0.02) derived here is in good agreement with the value of 0.25 (±0.02) from Hatakeyama *et al.*[28] from determination of H_2SO_4 production relative to ozone loss in chamber experiments, and considerably lower than the value of 0.44 from Horie and Moortgat,[41] derived from analysis of carbonyl products from the propene–ozone reaction. For 2-methylpropene, Hatakeyama *et al.*[28] derived a value of 0.17 (±0.03), using the method described above, compared to our value of 0.21 (±0.04).

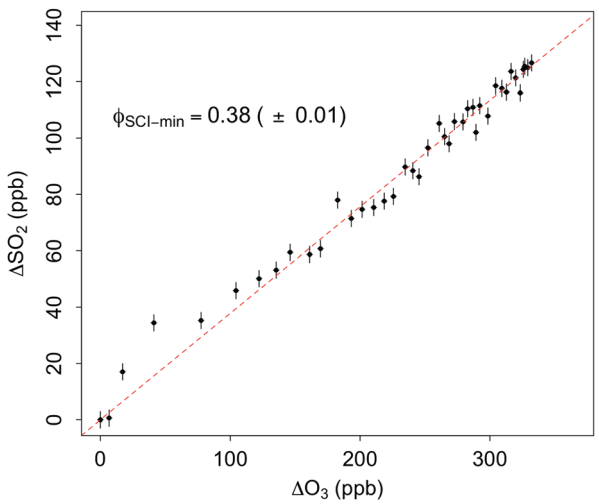

Fig. 1 Total SCI yield ($\phi_{SCI\text{-}min}$) in 2,4-dimethyl pent-2-ene ozonolysis, derived from the removal of SO_2 (ΔSO_2) relative to the removal of ozone (ΔO_3) (eqn (E1)). Dashed line: linear regression of measurements. Data is not corrected for additional loss processes – see text for details. Vertical and horizontal error bars represent precision uncertainties.

Table 1 Total SCI yields from the ten alkenes studied in this work. Uncertainties are $\pm 2\sigma$, and represent the combined systematic (estimated measurement uncertainty) and precision components

Alkene	SCI yield[a]	Literature values	Method
Ethene (C_2)	0.43 ($\pm$0.02)	0.35–0.54 (see Newland *et al.*;[31] Alam *et al.*[36] for refs)	
Propene (C_3)	0.34 ($\pm$0.01)	0.25 ($\pm$0.02)[28]	$\Delta H_2SO_4/\Delta O_3$
		0.44[41]	Carbonyl product yields
2-Methylpropene (C_4)	0.24 ($\pm$0.03)	0.17 ($\pm$0.03)[28]	$\Delta H_2SO_4/\Delta O_3$
2-Methyl-but-1-ene (C_5)	0.33 ($\pm$0.01)		
1-Heptene (C_7)	0.61 ($\pm$0.03)		
2-Methyl-but-2-ene (C_5)	0.28 ($\pm$0.01)		
2,3-Dimethyl-but-2-ene (C_6)	0.31 ($\pm$0.04)	0.10–0.65 (see Newland *et al.*[31] for refs)	
2,4-Dimethyl-pent-2-ene (C_7)	0.41 ($\pm$0.01)		
2,3,4-Trimethyl-pent-2-ene (C_8)	0.49 ($\pm$0.01)		
Myrcene (C_{10})	0.46 ($\pm$0.03)	0.35[42]	Theoretical calculations

[a] Uncertainties are $\pm 2\sigma$ and represent the combined systematic (estimated measurement uncertainty) and precision components.

Deng *et al.*[42] recently reported a total SCI yield of 0.35 for the monoterpene myrcene based on theoretical calculations (82% $(CH_3)_2COO$, 15% large *anti*-SCI, 3% large *syn*-SCI), compared to our measured value of 0.46. It may be expected that our experimental yield is an underestimation due to the very fast unimolecular reaction of the large *anti*-SCI formed in this system (calculated by Deng *et al.*[42] to be 7600 s^{-1}) which means that probably $<50\%$ would be scavenged by 2000 ppbv SO_2. Based on the yield of *anti*-SCI predicted by Deng *et al.*[42] (15%), this may lead to an underestimation of the total SCI yield of $\sim 8\%$. None of the other alkenes studied here have had total SCI yields reported previously to the authors' knowledge.

Fig. 2 shows the total SCI yields measured in this study plotted against carbon number of the parent alkene. Previous studies[43] have noted that total SCI yields do not appear to display a strong dependence on alkene size. The systems studied here suggest a weak dependence on the size of the parent alkene, with total SCI yield increasing with alkene size. Propene and 2-methylpropene have total SCI yields of 0.24–0.34, while the larger trisubstituted alkenes, 2,3,4 trimethyl-pent-2-ene and myrcene have yields of 0.41–0.49, and the largest terminal alkene, 1-heptene has a yield of 0.61 ($\pm$0.03). However, as shown later the total SCI yield is the product of a number of effects and hence any simple relation to alkene size must be treated with caution.

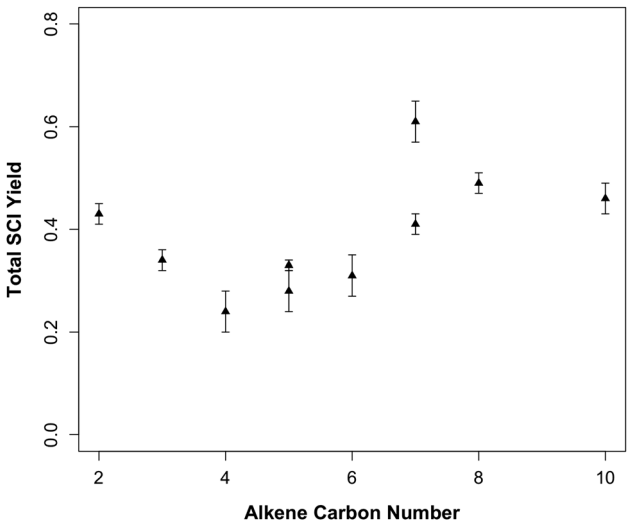

Fig. 2 Total SCI yields derived from ten alkene–ozone systems in this work.

Primary carbonyl yields

For non-symmetrical, non-cyclic, alkenes, a pair of CI and carbonyl co-products are formed in the decomposition of the POZ (Scheme 1). The sum yield of pathways $\alpha_1 + \alpha_2$ (*i.e.* the sum yield of the two possible primary carbonyls) should be equal to one. This has been confirmed to be the case in the extensive experimental dataset of Grosjean and Grosjean[44] for systems in which the smaller carbonyl is not also formed from decomposition of the larger CI. Therefore, by determining the yield of just one of the carbonyls (ideally the larger one, as it cannot be formed in CI decomposition) it is possible to determine both the primary yield of the other carbonyl, and the yield of both CI. For most CI, *syn* and *anti* conformers can also be formed because of the negligible rotation about the C=O bond of the CI moiety (Vereecken and Francisco, 2012). However, the two CI of focus in this study, CH_2OO and $(CH_3)_2COO$, are both symmetrical.

The relative magnitude of pathways α_1 and α_2 is determined by the fragmentation of the POZ. This appears to be determined predominantly by the structure around the double bond at which ozonolysis occurs.[3,45] A fraction, S, of each of the two CI formed is stabilised, either due to being formed below the energy threshold for being chemically activated, or *via* collisional stabilisation. The yield of each SCI is thus given by the product of α_i and S_i (eqn (E2); Scheme 1). The total yield of SCI from a given alkene is then the sum of the yields of the two specific SCI (eqn (E3)).

$$\phi_{\text{SCI-min}} = \alpha \times S \quad \text{(E2)}$$

$$\phi_{\text{SCI-tot}} = \alpha_1 \times S_1 + \alpha_2 \times S_2 \quad \text{(E3)}$$

The primary carbonyl yields in these experiments were determined by FTIR measurement of the yield of the primary carbonyls relative to the loss of ozone (both corrected for chamber dilution) (eqn (E4)).

$$\phi_{\text{carb-1}^\circ} = \frac{\Delta\text{carbonyl}}{\Delta O_3} \quad \text{(E4)}$$

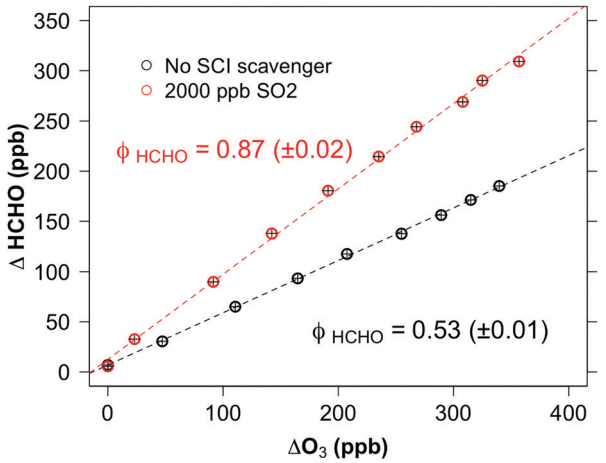

Fig. 3 Measured ΔHCHO *vs.* ΔO_3 (both corrected for dilution) for a hept-1-ene ozonolysis experiment with and without 2000 ppbv of the SCI scavenger SO_2 present. Precision uncertainties are smaller than the presented data points.

Fig. 3 shows an example of two experiments with 1-heptene, in the presence and absence of SO_2. The measured HCHO is plotted against ozone consumption (both corrected for chamber dilution). The HCHO yield of 0.52 (±0.01) in the zero SO_2 experiment, represents the primary HCHO. The HCHO yield is considerably higher in the SO_2 scavenger experiment (0.85 (±0.03)), because it is the sum of primary HCHO and secondary HCHO formed from the reaction of stabilised CH_2OO with SO_2 (reaction (R1)).

$$CH_2OO + SO_2 \rightarrow HCHO + SO_3 \quad (R1)$$

Table 2 shows the primary carbonyl yields determined for each alkene ozonolysis system studied. α_1 is the pathway that leads to the CI being studied here, *i.e.* CH_2OO or $(CH_3)_2COO$. Fig. S2 (ESI†) shows plots of the primary carbonyl yields for all experiments.

For alkenes in which HCHO or acetone are expected to be formed in the decomposition of the larger CI, α_1 was determined based on the measured yield of the larger carbonyl. HCHO is expected to be a decomposition product of any CI with a methyl group *syn* or *anti* to the carbonyl oxide moiety.[46] For *syn*-CI this comes *via* decomposition of a β-oxo-alkoxy radical formed *via* the vinyl-hydroperoxide mechanism; for *anti*-CI the methyl radical is formed in decomposition of a bis-oxy radical, formed *via* 1,3 ring closure of the CI, leading to CH_3O_2 and ultimately to HCHO. For longer alkyl chains, HCHO is not expected to be formed. For short chain terminal alkenes this is consistent with the extensive database of ozonolysis experiments by Grosjean and Grosjean[44] (and references therein). These show total primary carbonyl yields of unity for straight chain terminal alkenes with the exception of propene (that forms CH_3CHOO), for which the sum carbonyl yield is well in excess of 1 (1.30). Any alkene that produces $(CH_3)_2COO$ will also have a large secondary HCHO yield from decomposition of this CI.

CI stabilisation

The stabilisation, S, of a given CI is calculated as the ratio of the yield, ϕ, of the SCI to the yield of the CI (eqn (E5)). ϕ_{CI} is calculated as described above, based on the primary carbonyl yields in experiments with no SCI scavenger. ϕ_{SCI} for a specific CI is determined from the difference between the carbonyl yields in experiments with and without an SCI scavenger. The calculated stabilisation of CH_2OO and $(CH_3)_2COO$ in the alkene systems studied here are given in Table 3.

$$S = \frac{\phi_{SCI}}{\phi_{CI}} = \frac{\phi_{SCI}}{\alpha} = \frac{\phi_{carb\ 2^\circ} - \phi_{carb\ 1^\circ}}{\phi_{CI}} \quad (E5)$$

where carb 2° is the secondary yield of the carbonyl, *i.e.* from SCI + SO_2, and carb 1° is the primary yield of the carbonyl. For systems in which the carbonyl of interest (*i.e.* HCHO/acetone) could also be formed from decomposition of the larger CI, S is calculated by rearranging eqn (E3)–(E6).

$$S_1 = \frac{\phi_{SCI\text{-}tot} - (\alpha_2 \times S_2)}{\alpha_1} \quad (E6)$$

Table 2 Carbonyl yields and POZ decomposition branching ratios (α) from the ten alkenes studied here. The α_2 pathway leads to the CI being studied here, *i.e.* CH_2OO or $(CH_3)_2COO$. Carbonyl products were measured by FTIR. Uncertainties are ±2σ and represent the combined systematic (estimated measurement uncertainty) and precision components

	Zero SO_2		High SO_2			
Alkene	Carb1 yield	Carb2[a] yield	Carb1 yield	Carb2 yield	α_1	α_2
Carb1 = HCHO						
Ethene	—	—	1.31 (±0.07)	N.A.	1.00[b]	—
Propene	0.61 (±0.04)	0.38 (±0.06)	0.84 (±0.02)	0.62 (±0.02)	0.62	0.38
2-Methyl-but-1-ene	0.93 (±0.01)	0.40 (±0.01)	1.05 (±0.03)	0.50 (±0.01)	0.60	0.40
1-Heptene	0.53 (±0.01)	0.42 (±0.01)	0.84 (±0.03)	0.80 (±0.12)	0.53	0.47
Carb1 = Acetone						
2-Methylpropene	0.28 (±0.01)	1.19 (±0.04)	0.35 (±0.00)	1.26 (±0.02)	0.28	0.72
2-Methyl-but-2-ene	0.34 (±0.01)	0.80 (±0.07)	0.44 (±0.02)	0.69 (±0.12)	0.34	0.66
2,3-Dimethyl-but-2-ene	1.05 (±0.01)	—	1.38 (±0.05)	N.A.	1.00[b]	—
2,4-Dimethylpent-2-ene	0.22 (±0.01)	1.04 (±0.03)	0.50 (±0.02)	0.94 (±0.05)	0.22	0.78
2,3,4-Trimethylpent-2-ene	0.44 (±0.01)	0.78 (±0.01)	0.59 (±0.07)	0.72 (±0.08)	0.22	0.78
Myrcene	0.22 (±0.01)	—	0.61 (±0.03)	—	0.22	0.78

[a] Carb2 = the carbonyl formed from POZ decomposition that is not HCHO/acetone. [b] Assumed to be 1 by definition.

Table 3 Stabilisation of CH_2OO/$(CH_3)_2COO$ formed in the ten alkene systems studied. Calculated using either eqn (E5) and (E6) – see text for details. For ethene and 2,3-dimethyl-but-2-ene stabilisation of the CI is equal to the total SCI yield shown in Table 2

Alkene	Stab. (S)	Method
CH_2OO		
Ethene	0.43 (±0.02)	[a]
Propene	0.60 (±0.10)	[b]
2-Methylpropene	0.61 (±0.12)	(E6)
2-Methyl-but-1-ene	0.56 (±0.10)	(E6)
Hept-1-ene	0.73 (±0.08)	(E5)
$(CH_3)_2COO$		
2-Methylpropene	0.10 (±0.04)	(E5)
2-Methyl-but-2-ene	0.16 (±0.04)	(E5)
2,3-Dimethyl-but-2-ene	0.31 (±0.03)	[a]
2,4-Dimethylpent-2-ene	0.38 (±0.04)	(E5)
2,3,4-Trimethylpent-2-ene	0.53 (±0.04)	[b]
Myrcene	0.53 (±0.04)	(E5)

[a] Symmetrical, therefore total SCI yield (Table 2). [b] From model fit to data (Fig. S2, ESI).

where S_1 is the stabilisation of CH_2OO or $(CH_3)_2COO$, S_2 is the stabilisation of the other CI, calculated using eqn (E5).

Discussion

Fig. 4 shows the observed relationship between the stabilisation of the CI and the carbon number of the carbonyl co-product formed in POZ decomposition. There is a clear increase in stabilisation of both CH_2OO and $(CH_3)_2COO$ with increasing carbon number of the carbonyl co-product. This can be considered in terms of the distribution of the total energy available from decomposition of the POZ. If it is assumed that the total energy liberated in decomposition of the POZ is independent of the size of the alkene,[19] and that the available energy has time to become distributed equally between the non-hydrogen atoms (*i.e.* C and O), then as the size of the carbonyl co-product increases relative to the CI, so the proportion of the available energy that is taken by the CI will decrease. This would be expected to yield a CI population with a lower mean energy distribution, both increasing the yield of CI that are 'born cold', and also increasing the amount of CI that will be collisionally stabilised (Fig. 5). While theoretical work has shown that the energy distribution between CI and carbonyl fragments in POZ decomposition may be non-statistical,[47,48] it might still be expected that the general relationship will hold.

Based on the discussion above, the data presented in Fig. 4 can be fitted by the general relationship given in eqn (E7).

$$S = 1 - (A_{CI}/A_{tot}) \times F \quad \text{(E7)}$$

where A_{CI} is the number of non-hydrogen atoms (*i.e.* C and O) in the CI; A_{tot} is the total number of non-hydrogen atoms in the POZ; and F is a factor determined from the total SCI yield of the symmetrical alkene (*i.e.* ethene for CH_2OO and 2,3-dimethyl-but-2-ene for $(CH_3)_2COO$).

The relationship is plotted in Fig. 4 (red dashed line) for a SCI yield from ethene of 0.43 (lower limit of 0.39, upper limit of 0.43), and from 2,3-dimethyl-but-2-ene of 0.31 (0.27–0.35). It is seen that the prescribed relationship fits the observed data well. While there are certainly likely to be additional factors influencing the stabilisation of CI, such as specific substituents

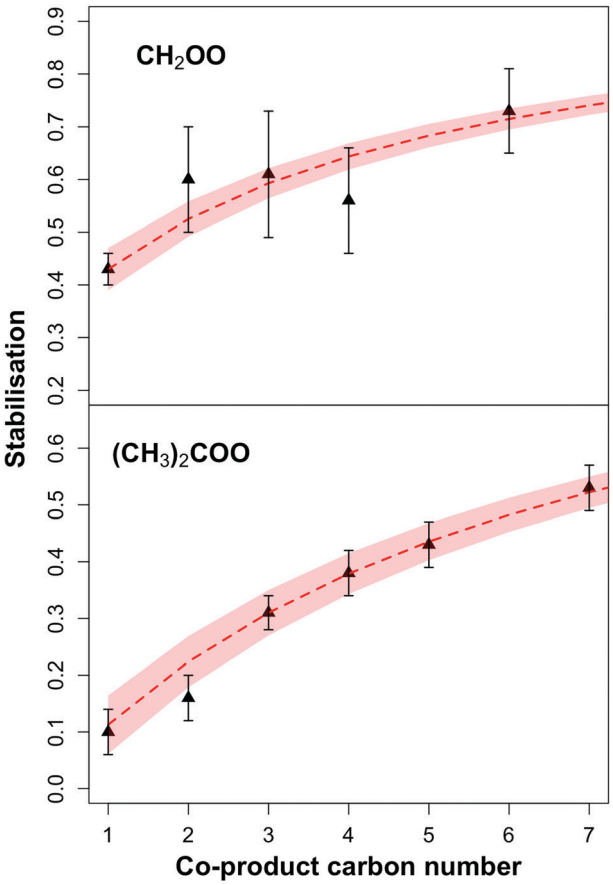

Fig. 4 Black triangles: variation of the stabilisation (S), of CH_2OO and $(CH_3)_2COO$ with size of carbonyl co-product determined from experiment. Red dashed line: modelled stabilisation using eqn (E7), assumes SCI yields of 0.43 (±0.04) and 0.31 (±0.04) for ethene (CH_2OO) and 2,3-dimethyl-but-2-ene ($(CH_3)_2COO$) respectively.

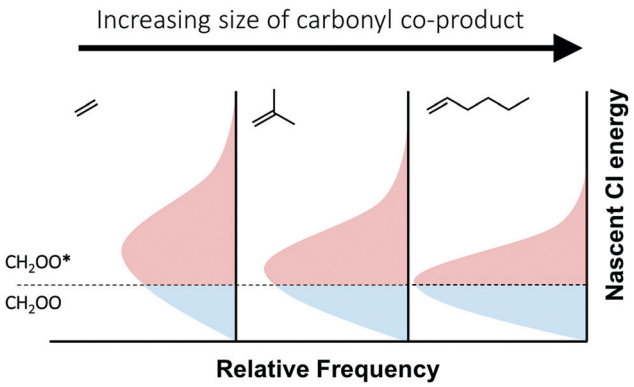

Fig. 5 Schematic showing the effect of increasing the size of the carbonyl co-product on the nascent mean energy distribution of a population of CI formed following POZ decomposition. As the mean energy decreases, the fraction of SCI increases.

and more complex structures, this work shows that the number of carbons in the system is a strong determinant of CI stabilisation, particularly for systems with similar structures.

For CI stabilisation from a given alkene, there is expected to be three important effects: (i) collisional stabilisation of the POZ, which will then decompose to yield exclusively stabilised CI – this has been predicted to be significant (65%) for the C_{15} sesquiterpene β-caryophyllene[49] but to be insignificant for smaller ($<C_{15}$) alkenes;[50] (ii) an increased stabilisation of a given CI with increasing parent alkene size, as shown herein; and (iii) an increased stabilisation of larger CI, which have longer lifetimes (due to distributing the initial energy from the POZ decomposition among a greater number of degrees of freedom) allowing greater collisional stabilisation.[20] This effect is particularly noticeable for 1-heptene in this dataset, with stabilisation of the larger CI, hexanal oxide being high ($\sim$50%).

Using the relationships shown here it is possible to calculate the stabilisation of a given CI produced from an alkene that also produces either CH_2OO or $(CH_3)_2COO$ if the total SCI yield and the POZ decomposition branching ratio (α) are known. However, there are still relatively few alkenes for which total SCI yields have been measured. Further useful information to inform structure activity relationships used in atmospheric models would cover: (i) the dependence of α on alkene structure; (ii) trends in the total SCI yields from symmetrical alkenes of increasing size and complexity, to provide values on which to pin the relationships observed herein; (iii) the effect of the size of the CI itself on stabilisation. In addition, information on the relative yields and stabilisation of (*E*)/(*Z*) CI is required to fully represent the impact of alkene ozonolysis on atmospheric composition. In addition to further experimental studies, a detailed theoretical study would provide strong corroborating evidence both for the relationship derived in this work, and the further work suggested here.

Atmospheric implications

This work suggests that small CI produced from large alkenes found in the atmosphere, *e.g.* isoprene, monoterpenes, sesquiterpenes, *etc.*, will predominantly be formed stabilised. For CH_2OO, the SCI of which reacts almost entirely with water vapour in the boundary layer, this will result in a high yield of the products of the $CH_2OO + H_2O/(H_2O)_2$ reaction, and low radical (OH and HO_2) yields (although it has been suggested that radical yields from CH_2OO decomposition are low anyway[51,52]). This finding is particularly important for isoprene, the most abundantly emitted alkene to the atmosphere.[53] Nguyen *et al.*[34] suggested that the total SCI yield ($\sim$0.6)[32–34] measured from isoprene ozonolysis is almost entirely stabilised CH_2OO (rather than the C_4-CI). The main products of the reaction of CH_2OO with water vapour are thought to be hydroxy-methylhydroperoxide (HMHP) and formic acid (HCOOH),[54] but recent flow tube experiments[55] suggest a roughly equal split between HMHP and formaldehyde (HCHO) from the $CH_2OO + (H_2O)_2$ reaction, with direct HCOOH formation $<$5%. The dominant fate of HMHP in the atmosphere is unclear, with a relatively long lifetime against reaction with OH of about 1 day.[56] OH reaction was shown to yield HCOOH and HCHO in a ratio of 0.88.[56] For $(CH_3)_2COO$, and other small *syn*-CI, for which reaction with water vapour is a negligible sink under boundary layer conditions,[55] a higher stabilisation will lead to an increased atmospheric concentration of these SCI. Under typical boundary layer conditions these SCI will participate in bimolecular reactions (*e.g.* with SO_2 and organic acids), contribute to aerosol formation, or undergo unimolecular decomposition.

Conclusions

Ozonolysis experiments were performed at the EUPHORE atmospheric simulation chamber on a range of alkenes that produce either the CH_2OO or $(CH_3)_2COO$ Criegee intermediates. Total stabilised Criegee intermediate (SCI) yields were determined from the temporal decay of the SCI scavenger SO_2. Speciated CI yields were determined based on FTIR measurements of primary carbonyl products. Speciated SCI yields were determined from comparison of carbonyl yields in the presence/absence of the SCI scavenger SO_2. From this information, the stabilisation of CH_2OO and $(CH_3)_2COO$ from each alkene was determined. The stabilisation is shown to increase with increasing carbon number of the carbonyl co-product formed in the decomposition of the primary ozonide. Stabilisation of CH_2OO increases from a minimum of $\sim$0.4 from ethene, to 0.71 from 1-heptene. Stabilisation of $(CH_3)_2COO$ increases from $<$0.1 from isobutene, to 0.50 from the monoterpene myrcene. An empirical relationship based on the energy distribution through the molecule on dissociation of the POZ fits the observed data well. This trend has implications for predicted tropospheric concentrations of SCI, with current models generally using SCI yields based on the total yield from the relevant symmetrical alkene–ozone system. From this work it is shown that stabilisation of small CI from many atmospherically relevant alkenes, such as isoprene and monoterpenes, is likely to be considerably higher than currently predicted. This would increase the importance of bimolecular reactions, and reduce radical yields from CI decomposition.

Data availability

Experimental data will be available in the Eurochamp database, www.eurochamp.org, from the H2020 EUROCHAMP2020 project, GA no. 730997.

Conflicts of interest

There are no conflicts to declare.

Acknowledgements

We would like to thank Luc Vereecken for very helpful discussions. The assistance of the EUPHORE staff is gratefully acknowledged. This work has received funding from the European Union's Horizon 2020 research and innovation programme through the EUROCHAMP-2020 Infrastructure Activity under grant agreement No. 730997, by means of its Transnational Activities,

and Fundacion CEAM and the Generalitat Valenciana for the IMAGINA-Prometeo project (PROMETEO2019/110). Fundación CEAM is partly supported by Generalitat Valenciana. Mike Newland and Andrew Rickard also acknowledge support from the Mechanisms for Atmospheric chemistry: GeneratioN, Interpretation and FidelitY – MAGNIFY project, funded by the UK Natural Environment Research Council (NERC, *via* grant NE/M013448/1). Beth Nelson acknowledges the NERC SPHERES Doctoral Training Partnership (DTP) for her studentship.

Notes and references

1 H. Niki, P. D. Maker, C. M. Savage, L. P. Breitenbach and M. D. Hurley, *J. Phys. Chem.*, 1987, **91**, 941–946.
2 S. E. Paulson and J. J. Orlando, *Geophys. Res. Lett.*, 1996, **23**, 3727–3730.
3 A. R. Rickard, D. Johnson, C. D. McGill and G. Marston, *J. Phys. Chem. A*, 1999, **103**, 7656–7664.
4 G. Salisbury, A. R. Rickard, P. S. Monks, B. J. Allan, S. J. B. Bauguitte, S. A. Penkett, N. Carslaw, A. C. Lewis, D. J. Creasey, D. E. Heard, P. J. Jacobs and J. D. Lee, *J. Geophys. Res.: Atmos.*, 2001, **106**, 12669–12687.
5 D. E. Heard, L. J. Carpenter, D. J. Creasey, J. R. Hopkins, J. D. Lee, A. C. Lewis, M. J. Pilling, P. W. Seakins, N. Carslaw and K. M. Emmerson, *Geophys. Res. Lett.*, 2004, **31**, L18112.
6 L. Vereecken, A. Novelli and D. Taraborrelli, *Phys. Chem. Chem. Phys.*, 2017, **19**, 31599–31612.
7 M. J. Newland, A. R. Rickard, T. Sherwen, M. J. Evans, L. Vereecken, A. Muñoz, M. Ródenas and W. J. Bloss, *Atmos. Chem. Phys.*, 2018, **18**, 6095–6120.
8 O. Welz, A. J. Eskola, L. Sheps, B. Rotavera, J. D. Savee, A. M. Scheer, D. L. Osborn, D. Lowe, A. Murray Booth, P. Xiao, M. Anwar, H. Kahn, C. J. Percival, D. E. Shallcross and C. A. Taatjes, *Angew. Chem., Int. Ed.*, 2014, **18**, 4547–4550.
9 F. A. Mackenzie-Rae, H. J. Wallis, A. R. Rickard, K. L. Pereira, S. M. Saunders, X. Wang and J. F. Hamilton, *Atmos. Chem. Phys.*, 2018, **18**, 4673–4693.
10 K. Kristensen, T. Cui, H. Zhang, A. Gold, M. Glasius and J. D. Surratt, *Atmos. Chem. Phys.*, 2014, **14**, 4201–4218.
11 X. Zhang, R. C. McVay, D. D. Huang, N. F. Dalleska, B. Aumont, R. C. Flagan and J. H. Seinfeld, *Proc. Natl. Acad. Sci. U. S. A.*, 2015, **46**, 14168–14173.
12 Y. Sakamoto, S. Inomata and J. Hirokawa, *J. Phys. Chem. A*, 2013, **117**, 12912–12921.
13 Y. Zhao, L. M. Wingen, V. Perraud, J. Greaves and B. J. Finlayson-Pitts, *Phys. Chem. Chem. Phys.*, 2015, **17**, 12500–12514.
14 M. Ehn, E. Kleist, H. Junninen, T. Petaja, G. Lonn, S. Schobesberger, M. Dal Maso, A. Trimborn, M. Kulmala, D. R. Worsnop, A. Wahner, J. Wildt and T. F. Mentel, *Atmos. Chem. Phys.*, 2012, **12**, 5113–5127.
15 J. R. Pierce, M. J. Evans, C. E. Scott, S. D. D'Andrea, D. K. Farmer, E. Swietlicki and D. V. Spracklen, *Atmos. Chem. Phys.*, 2013, **13**, 3163–3176.
16 T. Jokinen, T. Berndt, R. Makkonen, V. M. Kerminen, H. Junninen, P. Paasonen, F. Stratmann, H. Herrmann, A. B. Guenther, D. R. Worsnop, M. Kulmala, M. Ehn and M. Sipila, *Proc. Natl. Acad. Sci. U. S. A.*, 2015, **23**, 7123–7128.
17 R. Criegee and G. Wenner, *Liebigs Ann. Chem.*, 1949, **564**, 9–15.
18 D. Johnson and G. Marston, *Chem. Soc. Rev.*, 2008, **37**, 699–716.
19 L. Vereecken and J. S. Francisco, *Chem. Soc. Rev.*, 2012, **41**, 6259–6293.
20 G. T. Drozd and N. M. Donahue, *J. Phys. Chem. A*, 2011, **115**, 4381–4387.
21 M. Campos-Pineda and J. Zhang, *Chem. Phys. Lett.*, 2017, **683**, 647–652.
22 G. T. Drozd, T. Kurtén, N. M. Donahue and M. I. Lester, *J. Phys. Chem. A*, 2017, **121**, 6036–6045.
23 S. Hatakeyama and H. Akimoto, *Res. Chem. Intermed.*, 1994, **20**, 503–524.
24 G. T. Drozd, J. Kroll and N. M. Donahue, *J. Phys. Chem. A*, 2011, **115**, 161–166.
25 J. P. Hakala and N. M. Donahue, *J. Phys. Chem. A*, 2016, **14**, 2173–2178.
26 O. Welz, J. D. Savee, D. L. Osborn, S. S. Vasu, C. J. Percival, D. E. Shallcross and C. A. Taatjes, *Science*, 2012, **335**, 204–207.
27 H. Niki, P. D. Maker, C. M. Savage and L. P. Breitenbach, *Chem. Phys. Lett.*, 1977, **46**, 327–330.
28 S. Hatakeyama, H. Kobayashi and H. Akimoto, *J. Phys. Chem.*, 1984, **88**, 4736–4739.
29 T. Berndt, T. Jokinen, R. L. Mauldin III, T. Petaja, H. Herrmann, H. Junninen, P. Paasonen, D. R. Worsnop and M. Sipila, *J. Phys. Chem. Lett.*, 2012, **3**, 2892.
30 T. Berndt, T. Jokinen, M. Sipilä, R. L. Mauldin, H. Herrmann, F. Stratmann, H. Junninen and M. Kulmala, *Atoms. Environ.*, 2014, **89**, 603.
31 M. J. Newland, A. R. Rickard, M. S. Alam, L. Vereecken, A. Muñoz, M. Ródenas and W. J. Bloss, *Phys. Chem. Chem. Phys.*, 2015, **17**, 4076–4088.
32 M. Sipila, T. Jokinen, T. Berndt, S. Richters, R. Makkonen, N. M. Donahue, R. L. Mauldin III, T. Kurtén, P. Paasonen, N. Sarnela, M. Ehn, H. Junninen, M. P. Rissanen, J. Thornton, F. Stratmann, H. Herrmann, D. R. Worsnop, M. Kulmala, V. M. Kerminen and T. Petäjä, *Atmos. Chem. Phys.*, 2014, **14**, 12143–12153.
33 M. J. Newland, A. R. Rickard, L. Vereecken, A. Muñoz, M. Ródenas and W. J. Bloss, *Atmos. Chem. Phys.*, 2015, **15**, 9521–9536.
34 T. B. Nguyen, G. S. Tyndall, J. D. Crounse, A. P. Teng, K. H. Bates, R. H. Schwantes, M. M. Coggon, L. Zhang, P. Feiner, D. O. Milller, K. M. Skog, J. C. Rivera-Rios, M. Dorris, K. F. Olson, A. Koss, R. J. B. Wild, S. Stephen, A. H. Goldstein, J. A. de Gouw, W. H. Brune, F. N. Keutsch, J. H. Seinfeld and P. O. Wennberg, *Phys. Chem. Chem. Phys.*, 2016, **18**, 10241–10254.
35 K. H. Becker, EUPHORE: Final Report to the European Commission, Contract EV5V-CT92-0059, Bergische Universität Wuppertal, Germany, 1996.
36 M. S. Alam, M. Camredon, A. R. Rickard, T. Carr, K. P. Wyche, K. E. Hornsby, P. S. Monks and W. J. Bloss, *Phys. Chem. Chem. Phys.*, 2011, **13**, 11002–11015.
37 A. Muñoz, E. Borrás, M. Ródenas, T. Vera and H. A. Pedersen, *Environ. Sci. Technol.*, 2018, **52**, 9136–9144.

38 IUPAC Task Group on Atmospheric Chemical Kinetic Data Evaluation, http://iupac.pole-ether.fr.
39 R. M. I. Elsamra, A. Jalan, Z. J. Buras, J. E. Middaugh and W. H. Green, *Int. J. Chem. Kinet.*, 2016, **48**, 474–488.
40 A. Jalan, J. W. Allen and W. H. Green, *Phys. Chem. Chem. Phys.*, 2013, **15**, 16841–16852.
41 O. Horie and G. K. Moortgat, *Atmos. Environ., Part A*, 1991, **24**, 1881–1896.
42 P. Deng, L. Wang and L. Wang, *J. Phys. Chem. A*, 2018, **22**, 3013–3020.
43 M. E. Jenkin, S. M. Saunders and M. J. Pilling, *Atmos. Environ.*, 1997, **31**, 81–104.
44 E. Grosjean and D. Grosjean, *Environ. Sci. Technol.*, 1997, **31**, 2421–2427.
45 M. E. Jenkin, R. Valorso, B. Aumont, M. J. Newland and A. R. Rickard, *Atmos. Chem. Phys.*, 2020, in preparation.
46 E. C. Tuazon, S. M. Aschmann, J. Arey and R. Atkinson, *Environ. Sci. Technol.*, 1997, **31**, 3004–3009.
47 G. Vayner, S. V. Addepalli, K. Song and W. L. Hase, *J. Chem. Phys.*, 2006, **125**, 014317.
48 M. Pfeifle, Y.-T. Ma, A. W. Jasper, L. B. Harding, W. L. Hase and S. J. Klippenstein, *J. Chem. Phys.*, 2018, **148**, 174306.
49 T. L. Nguyen, R. Winterhalter, G. Moortgat, B. Kanawati, J. Peeters and L. Vereecken, *Phys. Chem. Chem. Phys.*, 2009, **11**, 4173–4183.
50 N. M. Donahue, G. T. Drozd, S. A. Epstein, A. A. Presto and J. H. Kroll, *Phys. Chem. Chem. Phys.*, 2011, **13**, 10848–10857.
51 T. L. Nguyen, H. Lee, D. A. Matthews, M. C. McCarthy and J. F. Stanton, *J. Phys. Chem. A*, 2015, **119**, 5524–5533.
52 D. Stone, K. Au, S. Sime, D. J. Medeiros, M. Blitz, P. W. Seakins, Z. Decker and L. Sheps, *Phys. Chem. Chem. Phys.*, 2018, **20**, 24940–24954.
53 K. Sindelarova, C. Granier, I. Bouarar, A. Guenther, S. Tilmes, T. Stavrakou, J.-F. Müller, U. Kuhn, P. Stefani and W. Knorr, *Atmos. Chem. Phys.*, 2014, **14**, 9317–9341.
54 P. Neeb, F. Sauer, O. Horie and G. K. Moortgat, *Atmos. Environ.*, 1997, **31**, 1417–1423.
55 L. Sheps, B. Rotavera, A. J. Eskola, D. L. Osborn, C. A. Taatjes, K. Au, D. E. Shallcross, M. A. H. Khan and C. J. Percival, *Phys. Chem. Chem. Phys.*, 2017, **19**, 21970–21979.
56 H. M. Allen, J. D. Crounse, K. H. Bates, A. P. Teng, M. P. Krawiec-Thayer, J. C. Rivera-Rios, F. N. Keutsch, J. M. St. Clair, T. F. Hanisco, K. H. Møller, H. G. Kjaergaard and P. O. Wennberg, *J. Phys. Chem. A*, 2018, **122**, 6292–6302.